ANALYSIS OF THE CARBON FIBER WING TORSION BOX AFTER LOW VELOCITY IMPACT DAMAGE

*I.A. Zharenov, *M.V. Pavlov

* TsAGI - Central Aerohydrodynamic Institute, Moscow distr., Russia

Abstract: *Composite products are gaining wide popularity in industrial production. But after getting impact damage composite parts do not behave as metals due to absence of plasticity. It is very important to analyze BVID damage and residual strength of the composite structure after impact damage.*

This problem is particularly critical for designing primary structures in aerospace industry. One of the most important elements of the airplane construction: carbon fiber wing torsion box was analyzed in this research.

The analysis was carried out on the damage after low velocity impact with use of Virtual Crack Closure Technique and Hashin criteria with corresponding degradation model. For detailed representation of stress fields submodeling technique was used as well.

Based on ABAQUS software all necessary engineering tools and complete approach to analyze composite structures were developed.

Keywords*: Composite Materials, residual strength, VCCT*

1. Introduction

In Aerospace industry is very important to deliver best safety of the primary structure as you can. For now you have an exact answer only in metal structures. So what happens if you are using composite primary structures? You have to take into account small defects after impact damage, because they are so dangerous in composite structures. In this paper presented method to solve a problem - residual strength and influence on the structure of the BVID after low velocity impact.

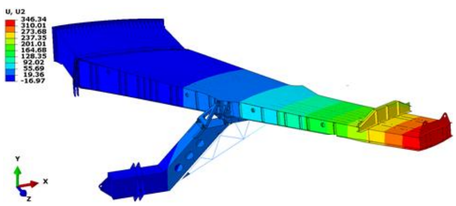

Figure 1 Prototype of the airplane wing

2. Theoretical part

Impact damage analysis was presented for the upper skin panel.

All parts in the analysis produced from carbon fiber reinforced composite material

For impact damage analysis Hashins criteria was used [2]. Dimensions of the delamination areas were determined with use of the Virtual Crack Closure Technique (VCCT) [3].

Margins of safety are defined from ply strengths and delamination strength of the structure components.
Ply strenght, K^H, defined based on the Hashins criteria. Hashin criteria have a good correlation with experimental data, and it distinguishes different modes of the destruction.
Residual strength coefficients are defined for four modes of ply damage:

$K_{XT} = 1/H_{XT}$, где $H_{XT} = \sqrt{\left(\frac{\sigma_{11}}{X^T}\right)^2 + \alpha\left(\frac{\tau_{12}}{S^L}\right)^2}$ - damage initiation index under fiber tension$(\sigma_{11} \geq 0)$;

$K_{XC} = 1/H_{XC}$, где $H_{XC} = \left|\frac{\sigma_{11}}{X^C}\right|$ damage initiation index under fiber compression$(\sigma_{11} < 0)$;

$K_{YT} = 1/H_{YT}$, где $H_{YT} = \sqrt{\left(\frac{\sigma_{22}}{Y^T}\right)^2 + \alpha\left(\frac{\tau_{12}}{S^L}\right)^2}$ damage initiation index under matrix tension$(\sigma_{22} \geq 0)$;

$K_{YC} = 1/H_{YC}$, где $H_{YC} = \sqrt{\left(\frac{\sigma_{22}}{2S^T}\right)^2 + \left[\left(\frac{Y^C}{2S^T}\right)^2 - 1\right]\frac{\sigma_{22}}{Y^C} + \left(\frac{\tau_{12}}{S^L}\right)^2}$ damage initiation index under matrix compression$(\sigma_{22} < 0)$.

Where
X^T – Longitudinal tension strength;
X^C - Longitudinal compression strength;
Y^T - Transverse tension strength;
Y^C - Transverse compression strength;
S^L - Longitudinal shear strength;
S^T- Transverse shear strength;
α - Shear stress contribution coefficient into fiber tension.

Damage initiation indexes showing material state under loading condition. How close material to fail under four different modes.

Fracture strength coefficients, K_G, are defined from:

1. If initiation of the delamination is under load lower than design load P^P, so
   $K_G = P^{in}/P^P$,
   where P^{in}- load of the initiation of the delamination.

2. If initiation of the delamination is under load more than design load P^P, so
$K_G = \sqrt{\frac{G_{equivC}}{G_{equiv}}}$,
where G_{equiv} - the equivalent strain energy release rate, G_{equivC} - the critical equivalent strain energy release rate.

3. FE model Upper skin panel

For the analysis was developed large scale global model of the prototype of the torsion wing box section (Figure 2). Local FE model of the upper skin panel was developed as well (Figure 3). Global model is loaded by design load. Sub model boundary conditions were used for the local model (Figure 4).

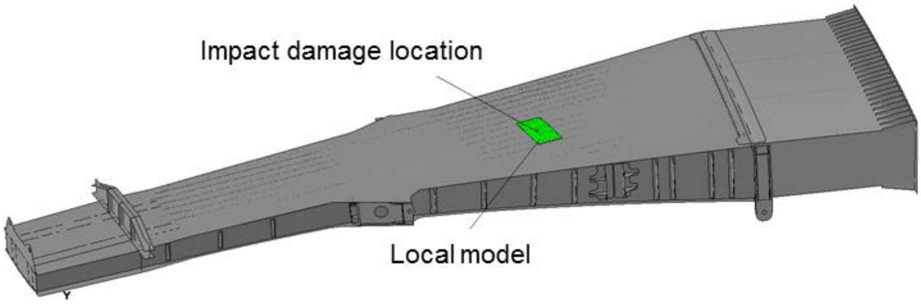

Figure 2 Global and local model

Figure 3 Local model of the upper skin panel

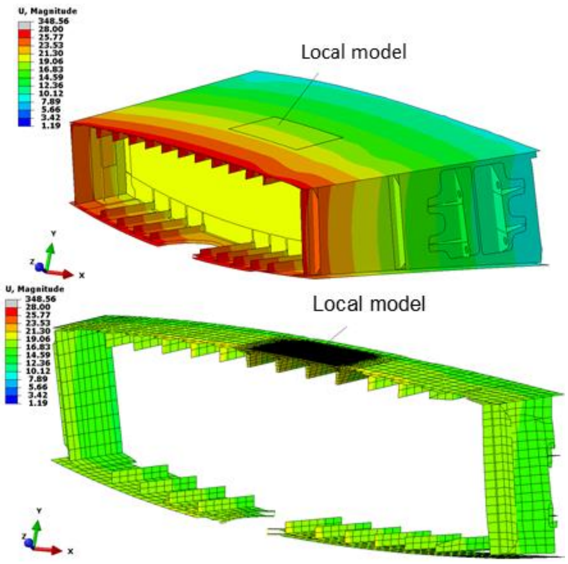

Figure 4 Sub model location with respect to global model

Stress components are calculated and shown in Figure 5. Damage initiation indexes are presented in Figure 6, Figure 7 as well.

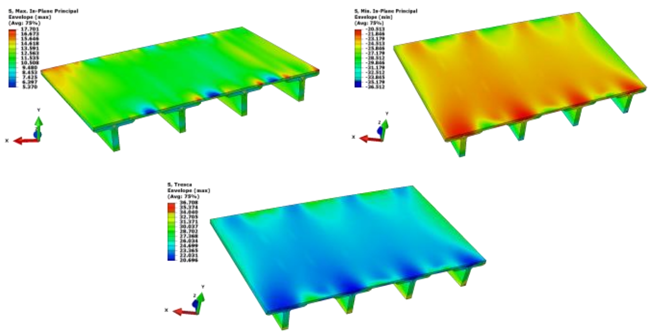

Figure 5 Max principal in-plane stress (left), min principal in-plane stress (center), Tresca shear stress (right)

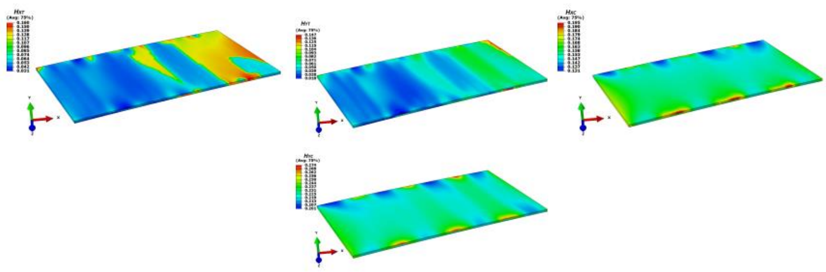

Figure 6 Damage initiation indexes of the skin without impact damage under loading

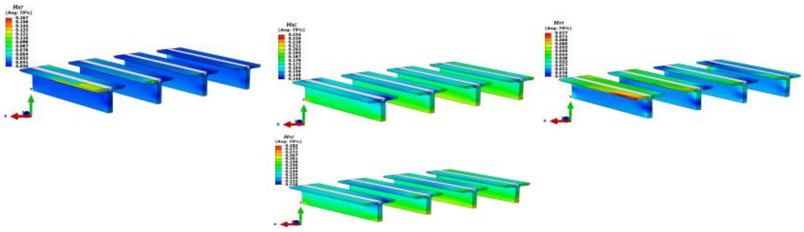

Figure 7 Damage initiation indexes of the stringers without impact damage under loading

Effective energy release rate ratio was obtained by VCCT method and is shown in Figure 8.

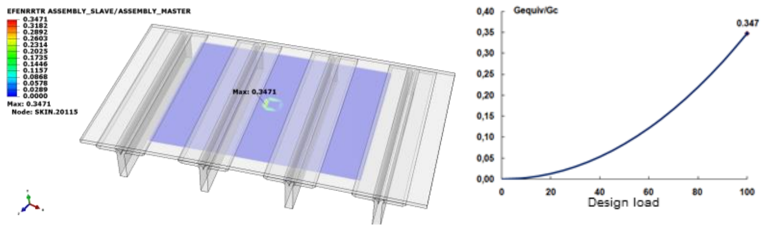

Figure 8 Effective energy release rate ratio (left), Gequiv/Gc vs design load (right)

4. Submodel impact damage. Impact energy 140 Joules

In this chapter FE model of the impact damage is presented. Rigid spherical impactor is pushed to the panel with different rate of impact energy. This analysis was done in Abaqus/Explicit[1]. In this work presented workflow for the impact energy 140 Joules, but the entire work was carried out for the 50, 90, 140, 200 and 240 Joules. And final results are shown for all energy values.

FE submodel of the reinforced upper skin panel is presented in Figure 9. In Figure 10 you can see maximum defect depth (maximum displacement, mm).

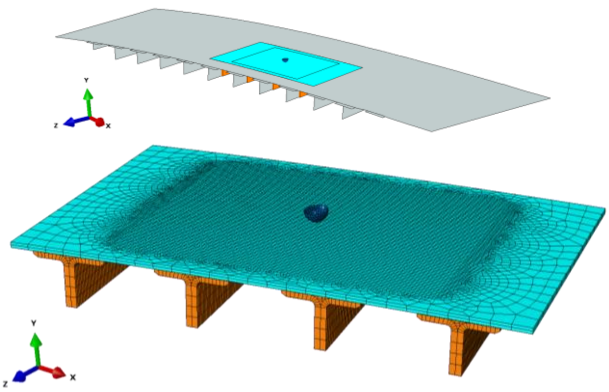

Figure 9 Global model and local model location (left), local FE model (right)

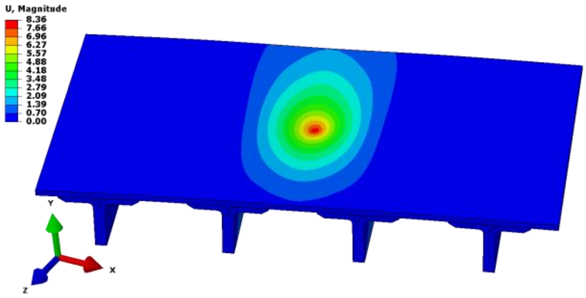

Figure 10 Maximum displacement after impact damage, impact energy 140J

Fields of properties degradation coefficients are presented in Figure 11, Figure 12, Figure 13. Delamination area is shown in Figure 14. And all data are tabulated in Table 1.

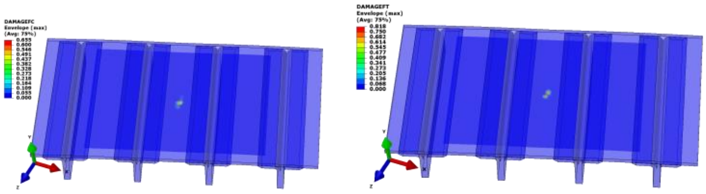

Figure 11 Fiber damage under compression (left), tension (right).

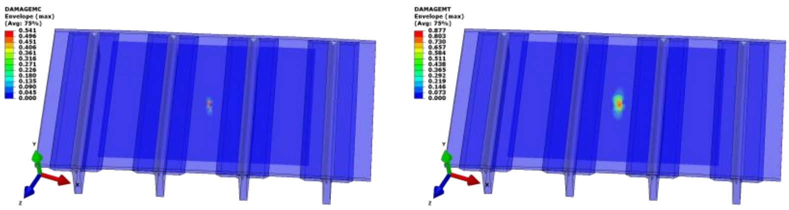

Figure 12 Matrix damage under compression (left), tension (right).

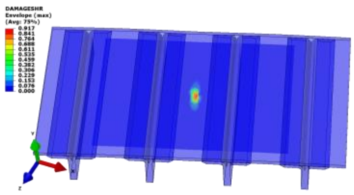

Figure 13 Matrix damage under shear

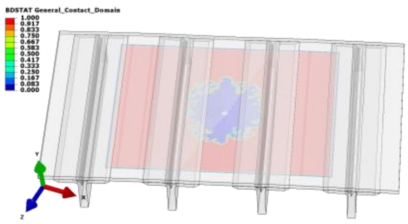

Figure 14 Delamination area

Table 1. Damage parameters

	d^c_f (fiber compression)	d^t_f (fiber tension)	d^c_m (matrix comp)	d^t_m (matrix tension)	d_s (shear)
Maximum	0.655	0.818	0.541	0.877	0.917
Average	0.328	0.409	0.271	0.439	0.459
Area of the damaged plies, mm^2	129	71	63	715	722
Delamination area, mm^2			15338		

5. Damaged material diagrams

Damage parameters were calculated for all energy rates and presented in Table 2. Graph representation is shown in Figure 15, Figure 16 and Figure 17.

S_{dam} – area of the material with degraded properties after impact,
S_{delam} – delamination area.

Table 2. Average values of the damage indexes and damaged material areas

Impact energy, J	d^c_f	d^t_f	d^c_m	d^t_m	d_s	S_{dam}, mm^2	S_{delam}, mm^2
50	0.201	0.252	0.064	0.385	0.426	226	6274
90	0.288	0.370	0.204	0.420	0.439	437	11161
140	0.328	0.409	0.271	0.439	0.459	722	15338
200	0.339	0.429	0.282	0.444	0.483	852	19079
240	0.352	0.438	0.298	0.452	0.487	946	20321

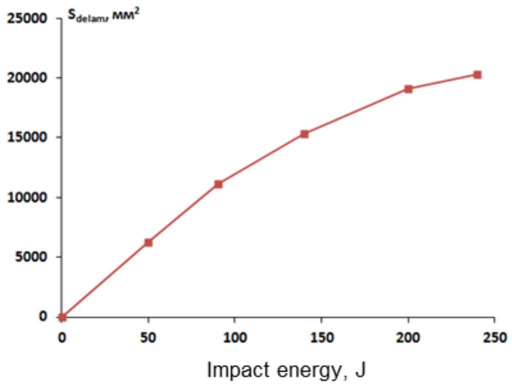

Figure 15 Delamination area versus impact energy

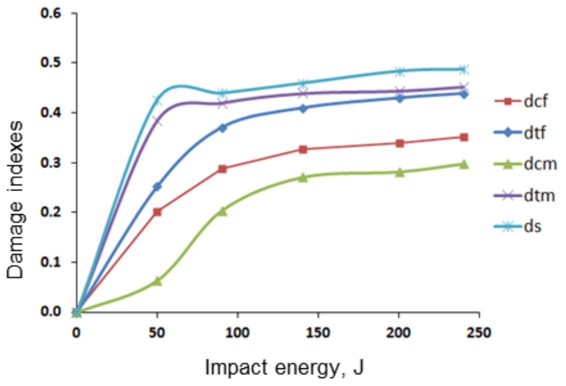

Figure 16 Damage indexes versus impact energy

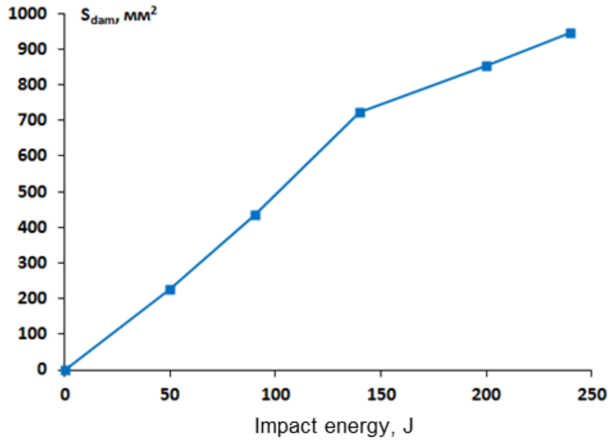

Figure 17 Area of the damaged ply material versus impact energy

6. Residual strength

In this part FE model for calculating the residual strength is presented in the Figure 18. Red area is the area of the material with degraded properties, 25mm*10mm.

Damaged material properties are presented in Table 3.

Table 3. Average properties of the damaged ply material

Parameters	Raw monopoly	Damaged material properties. Impact energy, J				
		50	90	140	200	240
E_1, kgs/mm^2	15200	11764.80	10203.00	9602.60	9367.00	9199.80
E_2, kgs/mm^2	846	656.07	582.26	546.09	538.90	528.75
G_{12}, kgs/mm^2	446	256.23	250.21	241.51	230.81	229.02
X^C, kgs/mm^2	156	124.72	111.07	104.91	103.12	101.17
X^T, kgs/mm^2	268	200.60	168.97	158.39	153.16	150.62
Y^C, kgs/mm^2	21.7	20.31	17.28	15.83	15.58	15.23
Y^T, kgs/mm^2	8.8	5.41	5.10	4.94	4.89	4.82
S, kgs/mm^2	8.4	4.83	4.71	4.55	4.35	4.31

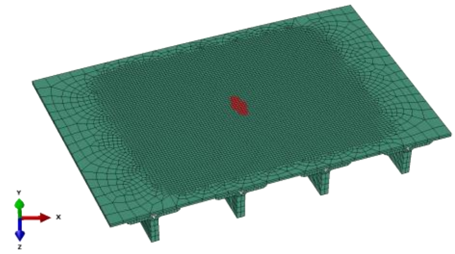

Figure 18 FE model for the residual strength calculation

7. Damageability energy is 140 Joules

Damage initiation indexes are presented in Figure 19, Figure 20. The values of the indexes are shown in Table 4.

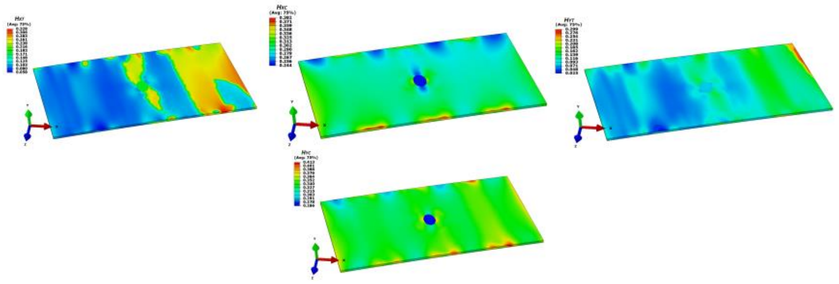

Figure 19 Damage initiation indexes of the skin with impact damage under loading, H_{XT}, H_{XC}, H_{YT}, H_{YC}

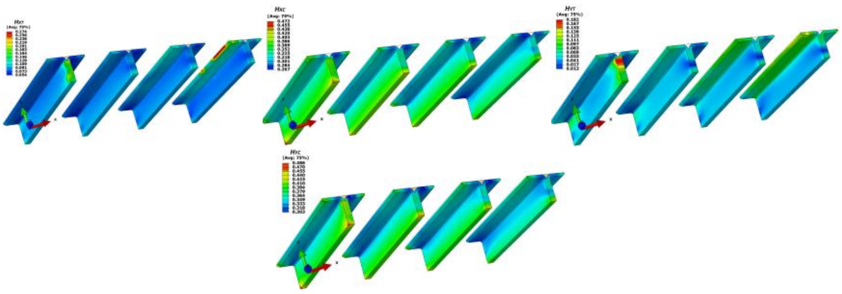

Figure 20 Damage initiation indexes of the stringer with impact damage under loading, H_{XT}, H_{XC}, H_{YT}, H_{YC}

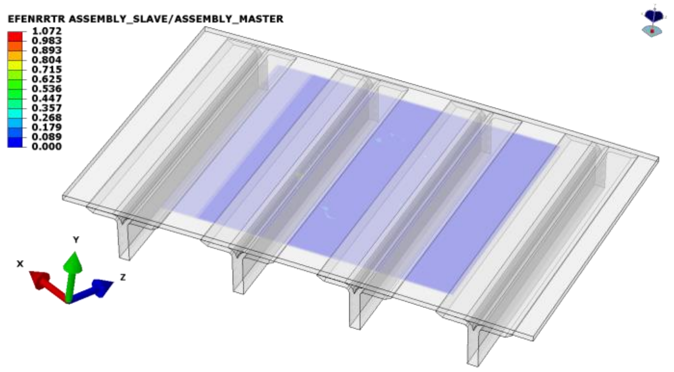

Figure 21 Effective Energy release rate ratio.

Effective energy release rate ratio field is shown in Figure 21. Two diagrams of the Effective Energy release rate ratio are shown in Figure 22.

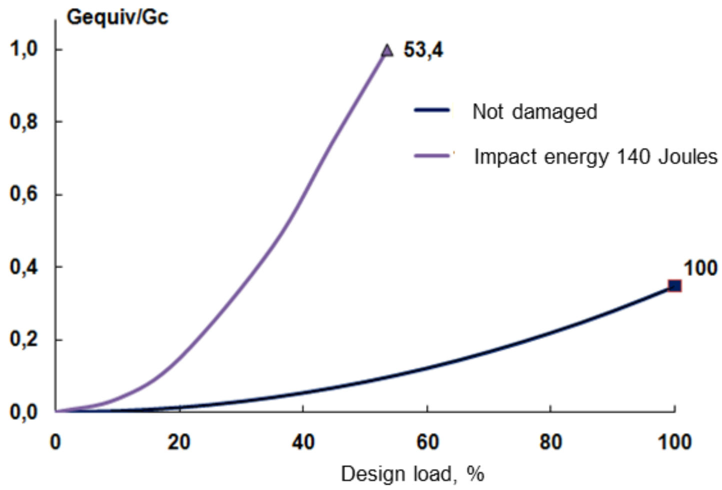

Figure 22 Gequiv/Gc versus design load for raw and damaged skin panel

Table 4. Damage initiation indexes and residual strength coefficients. Impact energy, 140 J

	H_{XT}	H_{XC}	H_{YT}	H_{YC}	K_{XT}	K_{XC}	K_{YT}	K_{YC}
Skin	0.328	0.382	0.299	0.413	3.049	2.618	3.344	2.421
Stringer	0.274	0.472	0.182	0.486	3.650	2.119	5.495	2.051
Minimal value, K	2.05							

Table 5 shows the residual strength value.

Table 5. Residual strength. Impact energy, 140 J

Delamination area	Residual strength
Skin	0.505

8. Residual strength diagrams

In this chapter residual strength diagram is presented. As described above, the same method was applied with different values of impact energy. Coefficients K_{ply} and K_{delam} are presented in Table 6. Graphical representation is shown in Figure 23.

K_{ply} – Strength coefficient of the ply,

K_{delam} – Fracture strength of the skin.

Table 6. Residual strength

Impact damage, Joules	K_{ply}	K_{delam}
0	3.53	1.76
50	3.29	0.94
90	2.16	0.71
140	2.05	0.505
200	1.72	0.33
240	1.50	0.30

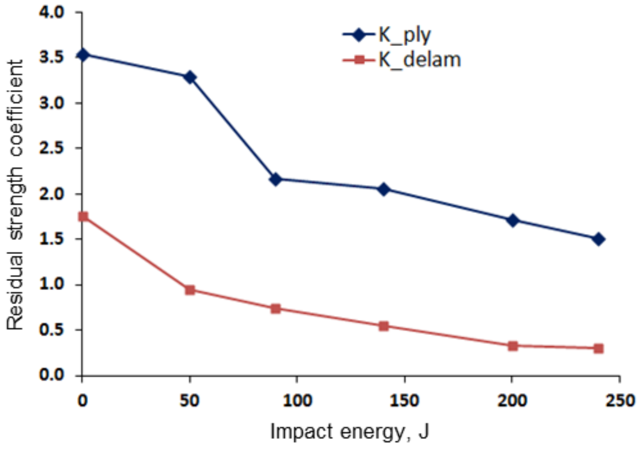

Figure 23 Residual strength versus impact energy diagram

9. Conclusions

The Abaqus software contributed greatly to solve this challenge. The Hashin criteria and VCCT allow developing this residual strength calculation method after low velocity impact– one of the most important tasks in aerospace industry.

10. References

1. Abaqus Users Manual, Version 6.12, Dassault Systémes Simulia Corp., Providence, RI.

2. Hashin Z. Failure Criteria for Unidirectional Fiber Composites. Journal of Applied Mechanics 1980;47:329-34.
3. Wu, E. M., and R. C. Reuter Jr., "Crack Extension in Fiberglass Reinforced Plastics," T and M Report, University of Illinois, vol. 275, 1965.